

# Rift propagation vs inherited crustal fabrics in the Trans-Mexican Volcanic Belt (Mexico): insights into geothermal investigations from analogue models

Daniele Maestrelli, Marco Bonini, Giacomo Corti, Domenico Montanari, and Giovanna Moratti

CNR-IGG The National Research Council of Italy, Institute of Geosciences and Earth Resources

[About the Authors](#)



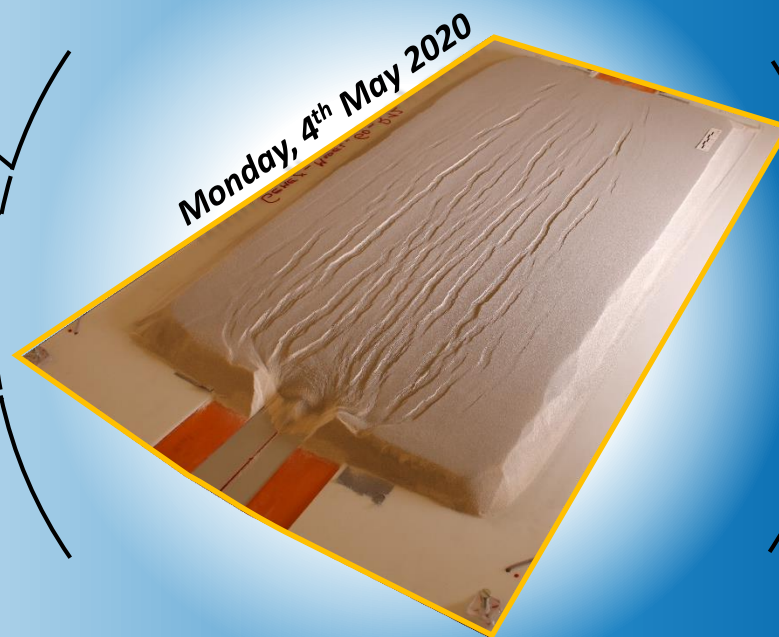
## INTRODUCTION & AIMS

### STUDY AREA

### SETUP

### EXPERIMENTAL SERIES

### MATERIALS AND SCALING



## ANALYSIS & RESULTS

### DISCUSSION

### COMPARISON WITH NATURE

### CONCLUSIONS

[Reference and acknowledgments](#)

#### NAVIGATION TOOLS

 «Home» button

 Clickable links

 Back

 Forward

- This work has been performed in the frame of the GEMex-project. GEMex aims to push forward geothermal exploitation (implementing EGS and SGS) at two sites in Mexico: Los Humeros and Acoculco volcanic complexes.
- This work is framed in the project due to the necessity to investigate also at a regional scale the possible interactions between volcanic features and tectonic elements.
- We aimed at the definition of the role of regional tectonics on the possible evolution of volcanic systems (e.g. Los Humeros and Acoculco calderas, under exploration for geothermal energy) in the Trans-Mexican Volcanic Belt (TMVB).
- We therefore performed analogue models to investigate the role of rift propagation vs inherited crustal fabrics. Structures prone to be reactivated during extension might, in fact, be preferential pathways for magma emplacement and volcanic localization, becoming therefore target for geothermal exploration.

## More about GEMex

*GEMex Project-Cooperation in Geothermal energy research Europe-Mexico for development of Enhanced Geothermal Systems and Superhot Geothermal Systems*

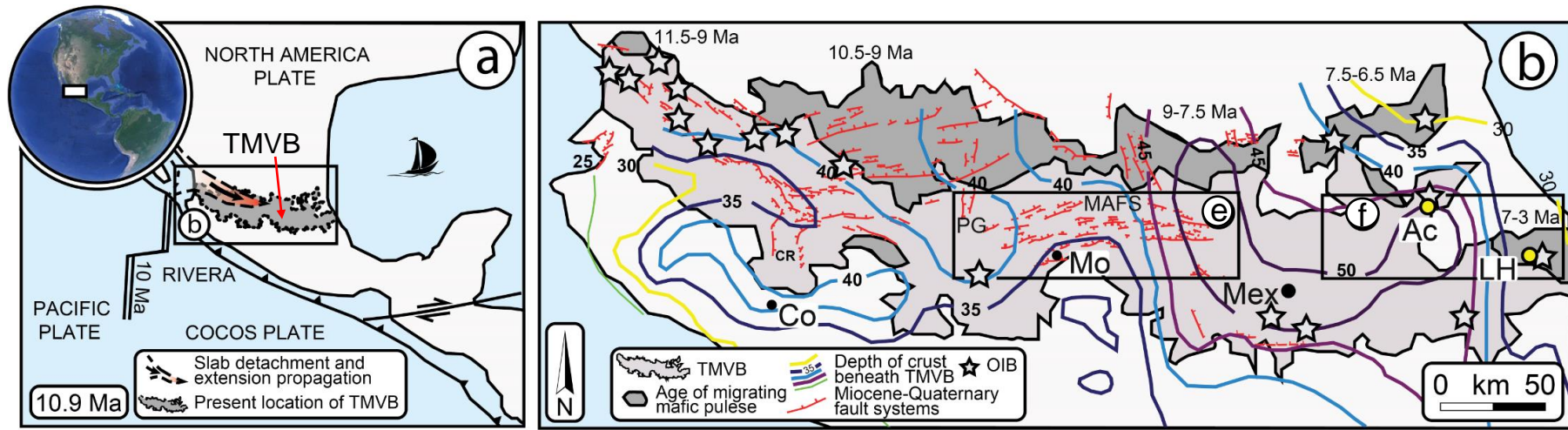


(H2020 Programme, grant agreement No. 727550).

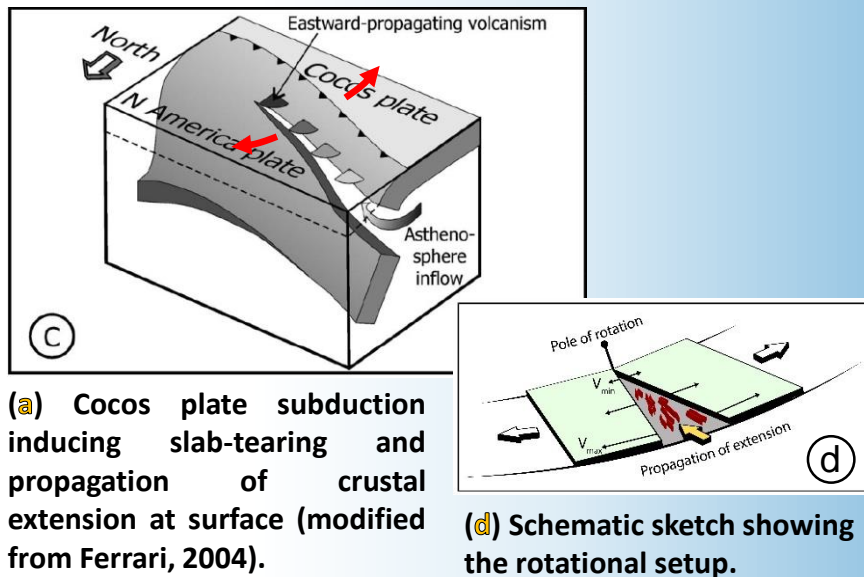


Bird's eye view of Iztaccíhuatl and Popocatepetl volcanoes, in the TMVB (16<sup>th</sup> October 2018)

# THE TRANS-MEXICAN VOLCANIC BELT



(a) Geodynamic setting of the TMVB and (b) its extension through the North America plate. The two insets (e,f) in b mark the position of the study areas. (modified from Maestrelli et al., submitted)



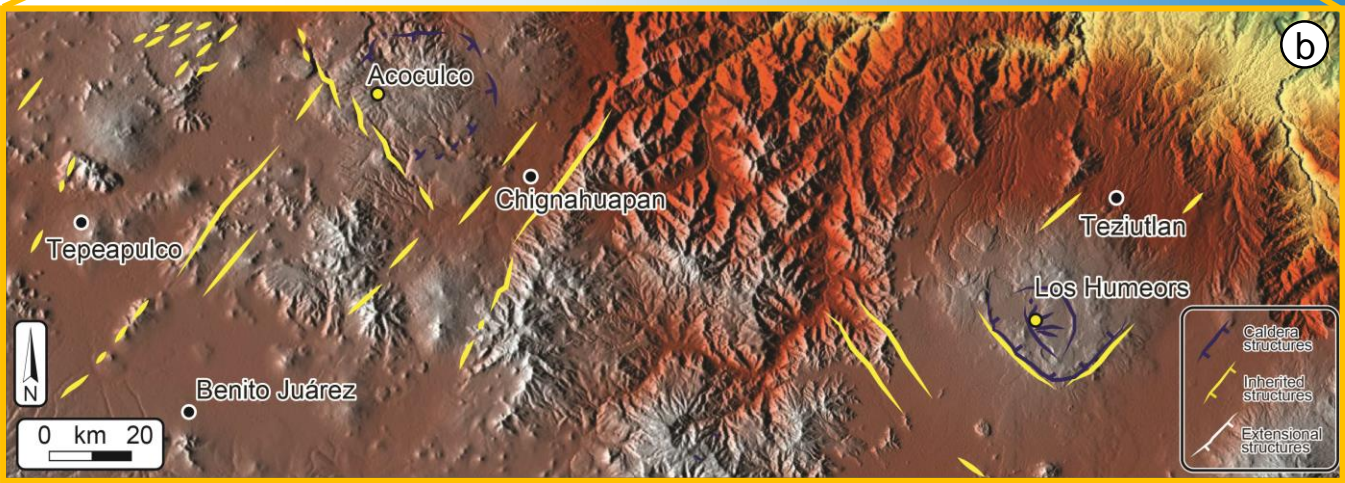
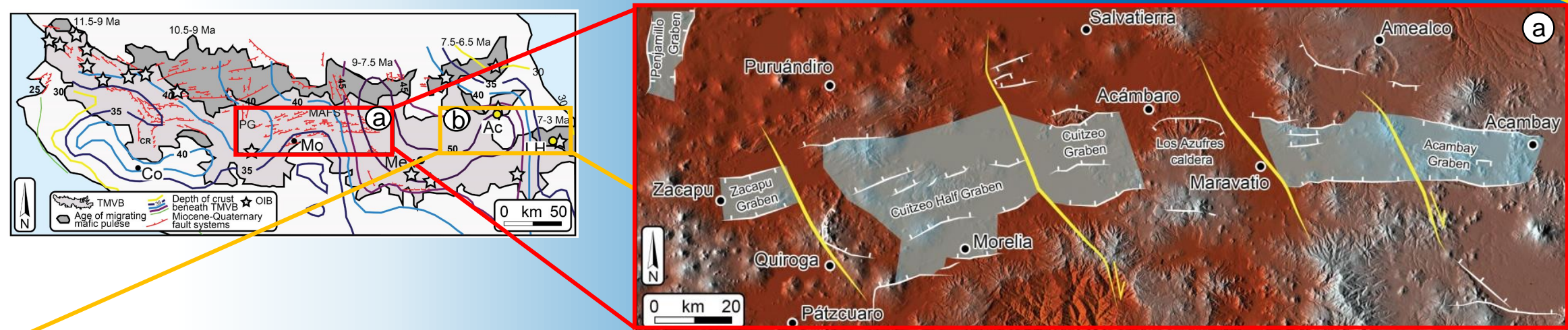
(a) Cocos plate subduction inducing slab-tearing and propagation of crustal extension at surface (modified from Ferrari, 2004).

(d) Schematic sketch showing the rotational setup.

- The Trans-Mexican Volcanic Belt (a,b; TMVB) is a large-scale, NW to SE trending volcano-tectonic feature extending through central Mexico for a length of more than 1000 km.
- In some models (a,c) its genesis is related to the interaction between the subducting Rivera and Cocos plates and the North America plate, with the eastward propagation of volcanism being associated with slab detachment and consequent asthenospheric upwelling (e.g., Ferrari, 2004).
- Progressive SE-directed slab tearing has been causing propagating crustal extension and the emplacement of large-scale volcano and caldera edifices (b).
- This process can be efficiently simulated in our model by reproducing a rotational tectonic setup (d).



# THE MORELIA-ACAMBAY FAULT SYSTEM AND LOS HUMEROS AND ACOCULCO CALDERAS



(a) The Morelia-Acambay Fault system (MAFS) in the central TMVB (modified from Maestrelli et al., submitted)

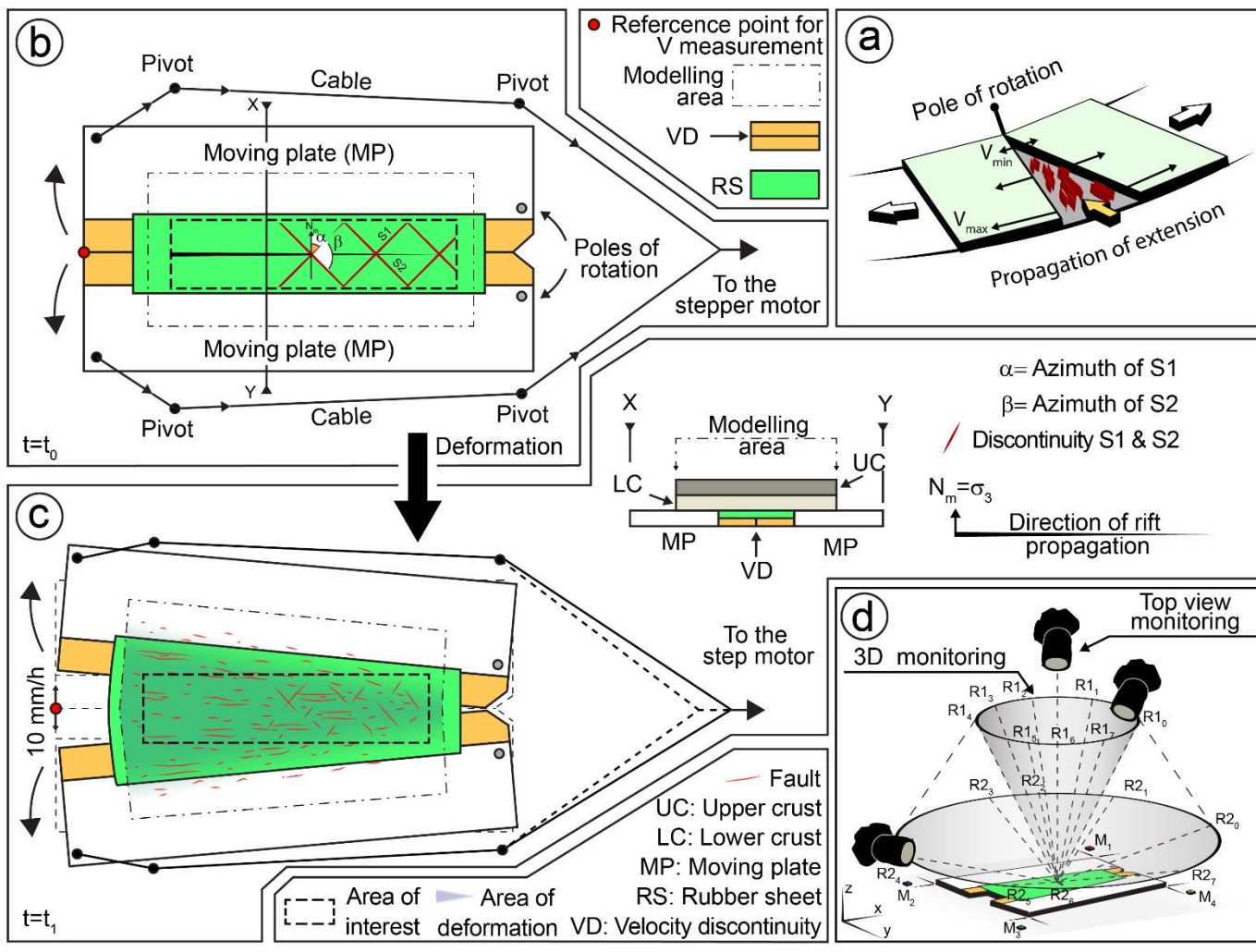
- The Morelia-Acambay Fault System (a; MAFS) is composed of W-E trending extensional faults which are offset by NW-SE inherited structure, at places reactivated as strike-slip faults.
- The area where Los Humeros (LH) and Acoculo (Ac) calderas are located (b; target of GEMex Project), shows NW-SE and NE-SW trending inherited structures, that are hypothesize to have played a role during the collapse of these caldera systems (Campos-Enriquez & Garduño-Monroy, 1987).

STUDY AREA

(b) The LH-Ac study area, showing in yellow inherited structures that likely influenced the caldera collapse. Faults are simplified from Avellán et al. (2019); García-Palomo et al. (2018) and Norini et al. (2019). (modified from Maestrelli et al., submitted)



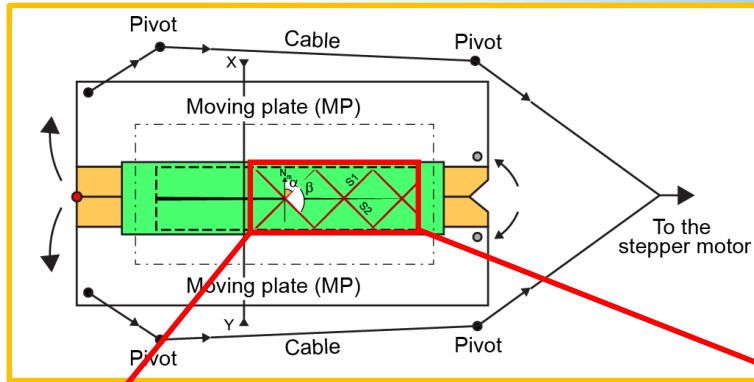
## ...INDUCING EXTENSION PROPAGATION



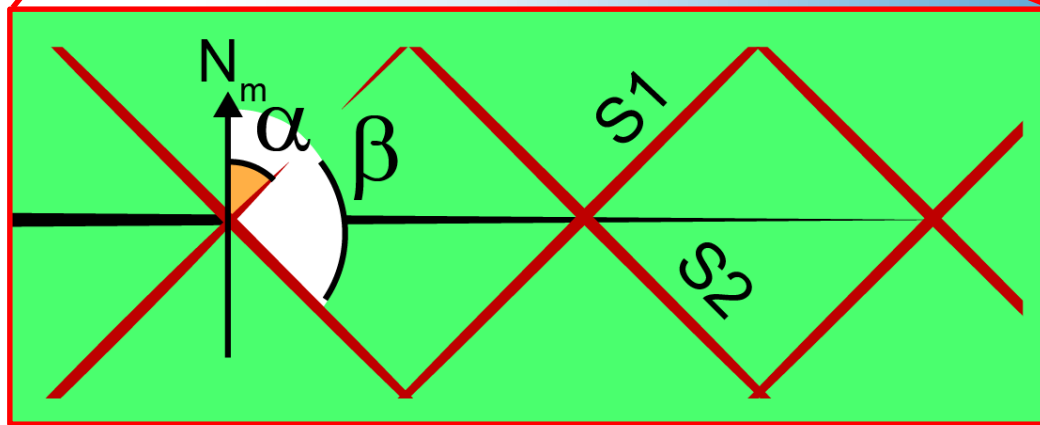
(a,b,c) The rotational tectonic setup used in this study. (d) Top view and 3D photo acquisition strategy applied to monitor model deformation (modified from Maestrelli et al., submitted).

- We built up a rotational tectonic setup (a) in order to induce rift propagation and reproduce the gradient of deformation observed in nature.
- The use of a basal Rubber Sheet (RS) allowed for distribution of deformation (a,c).
- A Lower Crust (LC, 1 cm-thick) layer is simulated by a PDMS-corundum sand mixture.
- An Upper Crust (LC, 1 cm-thick) layer is simulated using 70:30 (% wt) Qz-Kfeldspar sand mixture (see Montanari et al., 2017).
- Brittle discontinuities simulating natural faults are cut through the UC layer at various trending angles ( $\alpha$  and  $\beta$ , with respect to the North of the model; a).

## ...CUTTING BRITTLE DISCONTINUITIES



- Brittle discontinuities simulating natural faults are cut through the UC layer at various trending angles ( $\alpha$  and  $\beta$ , with respect to the North of the model, **a**).
- Sand was then poured and scraped (1 mm thick) to flatten the model surface and to better see whether discontinuities are reactivated during deformation (**b**).



**(a)** Orientation of discontinuity sets S1 and S2 with respect to the north of the model (modified from Maestrelli et al., submitted)



**(b)** Example of two discontinuity sets S1 and S2 cutting through the UC layer of a target model.

## 10 MODELS: DISCONTINUITIES VARIOUSLY TRENDING

Model	Azimuth of S1 ( $\alpha$ ) [°]	Azimuth of S2 ( $\beta$ ) [°]
RP-1	/	/
RP-2	30	/
RP-3	/	125
RP-4	30	125
RP-5	15	165
RP-6a	45	135
RP-6b	45	135
RP-7	60	120
RP-8	75	105
RP-9	90	180

Orientation of discontinuity sets S1 and S2 for each model (modified from Maestrelli et al., submitted)

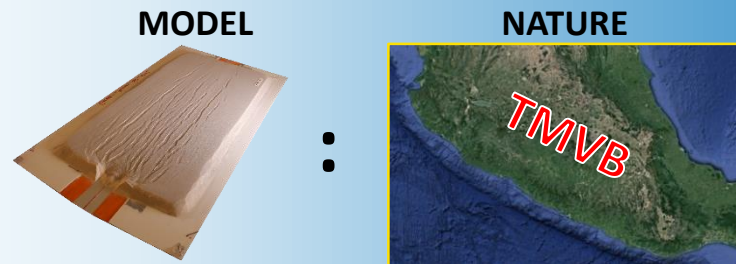
- We have selected 10 models (out of 30) that parametrically tested discontinuities with various trend.
- This was done to investigate the relationships between rift propagation and crustal fabrics in the frame of general perspective, and not only to apply and compare models to the specific natural case studies represented by the TMVB.
- NB: our models show similarities with many other natural prototypes...This aspect further is addressed in the submitted paper; see more at the end of this presentation!

- Model RP-6a and RP-6b showed different results with the same setup and therefore are both reported. A third model (RP-6c), not shown, provided the same result as Model RP-6b.

## ...SOME PARAMETERS

Analogue material & parameter		Model	Nature	Model/Nature ratio
<b>Qz-K-feldspar sand mixture</b> (80:20 % in weight) (simulates the Upper Crust - UC)	Density $\rho$ (kg m <sup>-3</sup> )	1440	~2700 (upper crust)	$\rho^* \sim 0.53$
	Internal friction coefficient $m$	0.81-1	0.85	$m^* \sim 1$
	Cohesion $c$ (Pa)	~6	~1x10 <sup>7</sup>	$c^* = 6 \times 10^{-7}$
	Thickness $h$ (m)	0.01	15000	$h^* = 6.67 \times 10^{-7}$
<b>PDMS-Corundum</b> (~ 1:1 % in weight) (simulates the Lower Crust - LU)	Density $r$ (kg m <sup>-3</sup> )	1440	~2700	$\rho^* = 0.53$
	Viscosity $\eta$ (Pa s)	1.69x10 <sup>5</sup>	10 <sup>22</sup>	$\eta^* = 1.69 \times 10^{-17}$
	Thickness $h$ (m)	0.01	15000	$h^* = 6.67 \times 10^{-7}$
<b>Length <math>l</math> (m)</b>		0.01	15000	$l^* = 6.67 \times 10^{-7}$
<b>Gravity <math>g</math> (m s<sup>-2</sup>)</b>		9.81	9.81	$g^* = 1$
<b>Stress <math>\sigma'</math> (Pa)</b>				$\sigma^* = 3.53 \times 10^{-7}$
<b>Strain rate <math>\dot{\epsilon}</math> (s<sup>-1</sup>)</b>		5.55x10 <sup>-4</sup>	2.66 x10 <sup>-14</sup>	$e^* = s^*/h^*$ $= 2.1 \times 10^{10}$
<b>Velocity <math>v</math> (m s<sup>-1</sup>)</b>		5.55x10 <sup>-6</sup>	3.99 10 <sup>-10</sup> (=12.5 mm yr <sup>-1</sup> )	$v^* = e^* l^* = 14000$

Materials and scaling ratio adopted for our models (modified from Maestrelli et al., submitted).



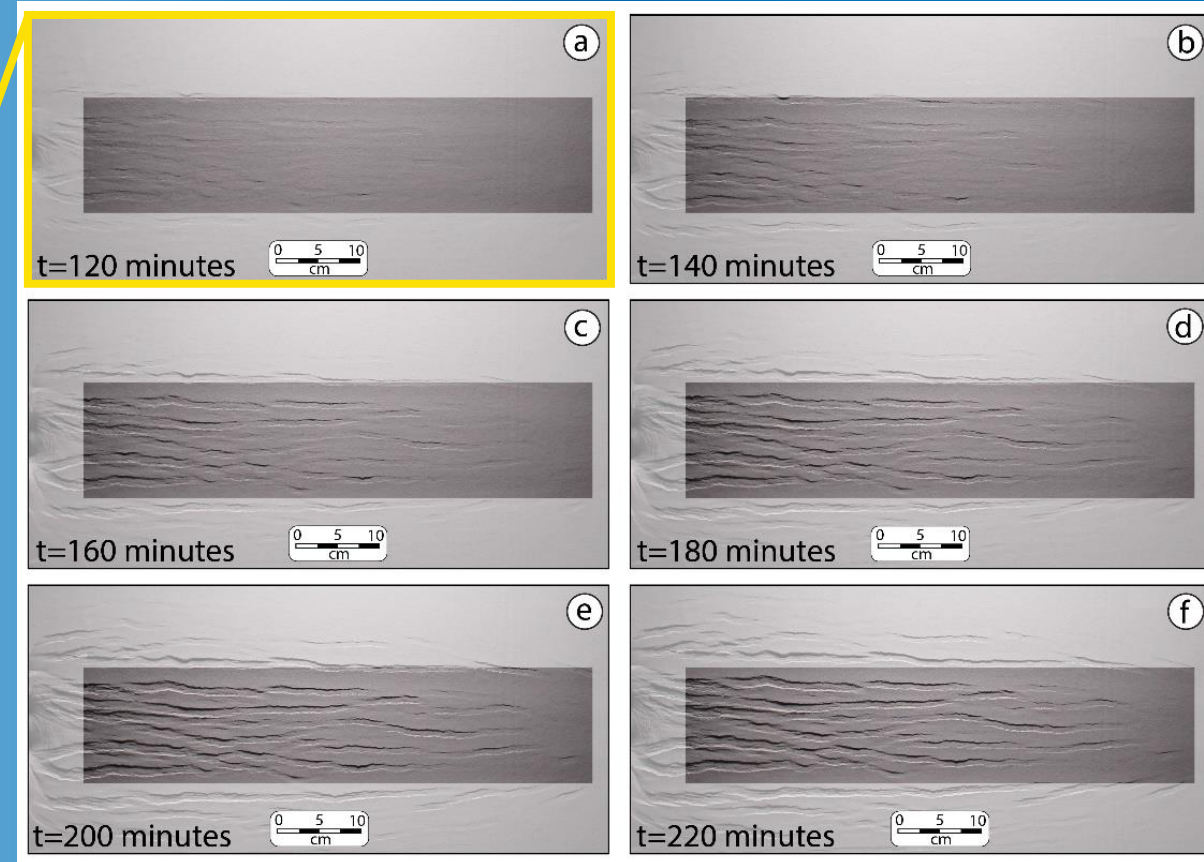
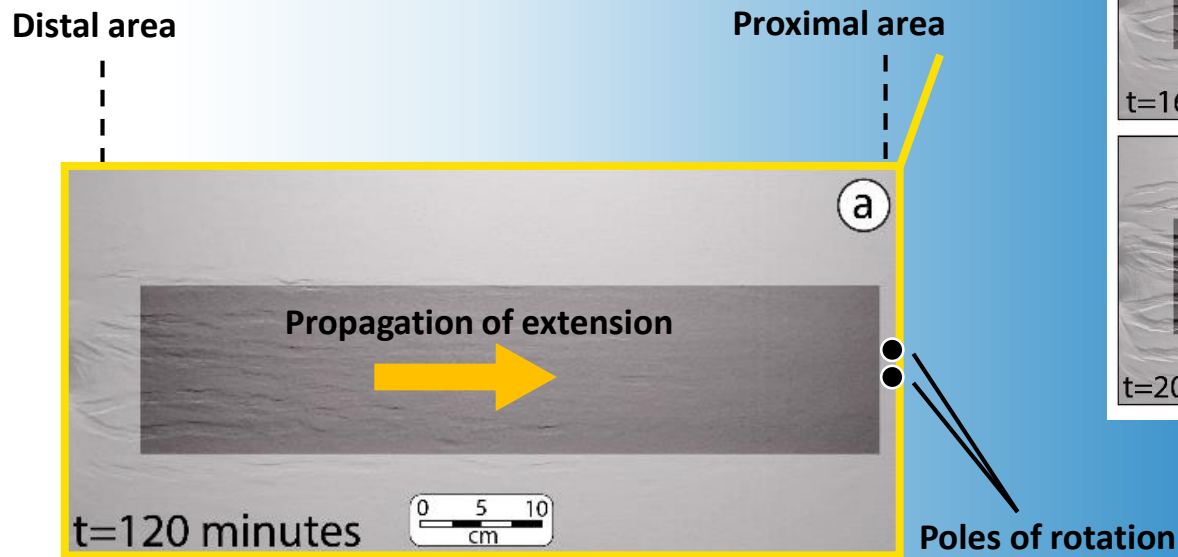
= 1 cm : 15 km

- A Lower Crust (LC, 1 cm-thick) layer is simulated by a PDMS-corundum sand mixture.
- An Upper Crust (LC, 1 cm-thick) layer is simulated using 70:30 (% wt) Qz-Kfeldspar sand mixture.
- The table shows the characteristics of experimental materials and the scaling ratios adopted for the analogue models. The asterisk (\*) denotes the ratio between model and nature for a given parameter. Characteristics of the granular material represented by the Qz-K-feldspar sand mixture are derived from Montanari et al. (2017) and Del Ventisette et al. (2019).
- In particular, the geometrical scaling ratio was ca.  $6.7 \times 10^{-7}$ , such that 1 cm in the models simulated 15 km in nature.



## REFERENCE MODEL (RP-1) :NO DISCONTINUITIES

- A first model (Model RP-1) was run with no discontinuity to be used as reference model.
- Deformation started in the distal area (a; i.e. opposite to the poles of rotation) and continued toward the poles of rotation (proximal area) to create a V-shaped pattern of deformation represented by E-W trending graben systems (b to f).

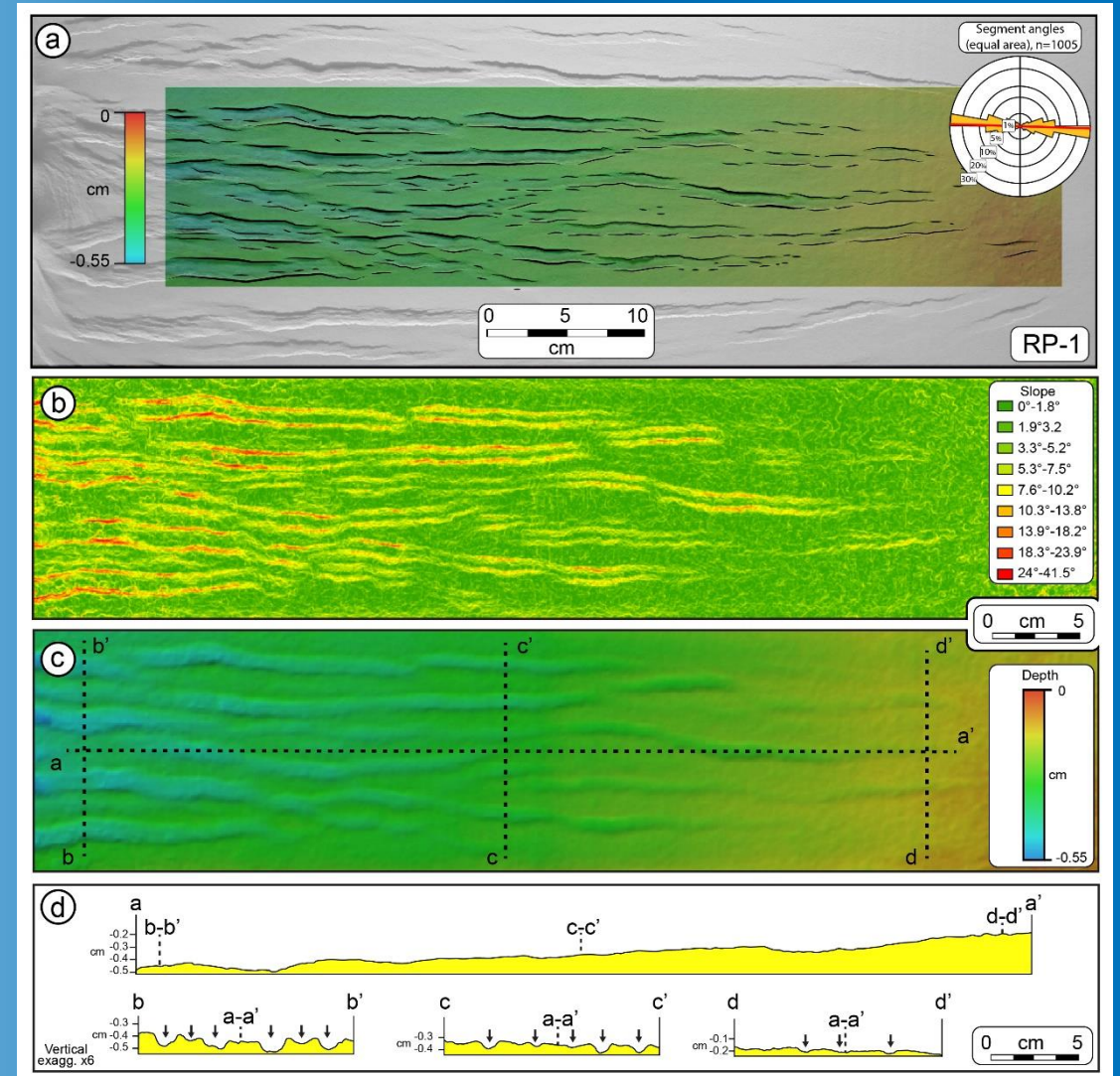


(a to f) ) Top view evolution of reference Model RP-1 (modified from Maestrelli et al., submitted)

## REFERENCE MODEL (RP-1) : NO DISCONTINUITIES

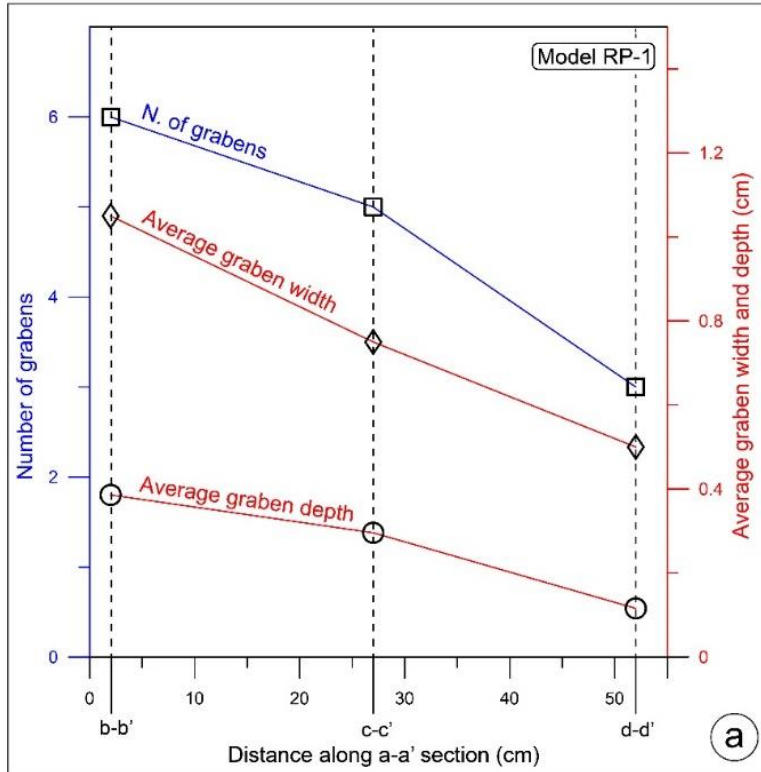
- The wedge of deformation propagates toward the poles of rotation (a) and incrementally increases the number, length and vertical throw of the faults. These observations are supported by slope analysis performed on the DEM obtained for the final deformation stage (b).
- Interestingly, steeper scarps localize in the distal area as result of a larger bulk deformation, this also being the area where fault density is higher. Closer to the poles of rotation, vertical fault throw is smaller, similar to the slope of the fault scarps (b,c). This is particularly evident comparing topographic profiles obtained from model DEM (d).
- Profile a-a' shows, in fact, a gradual decrease of elevation from the proximal area toward the distal area, with a variation of surface elevation ( $\Delta d$ ) of about 3 mm (see section a-a' in c).

(a) Top-view interpretation (superimposed on DEM) of Model RP-1 and (b) its slope analysis. (c) Trace of topographic profiles shown in (d) (modified from Maestrelli et al., submitted).

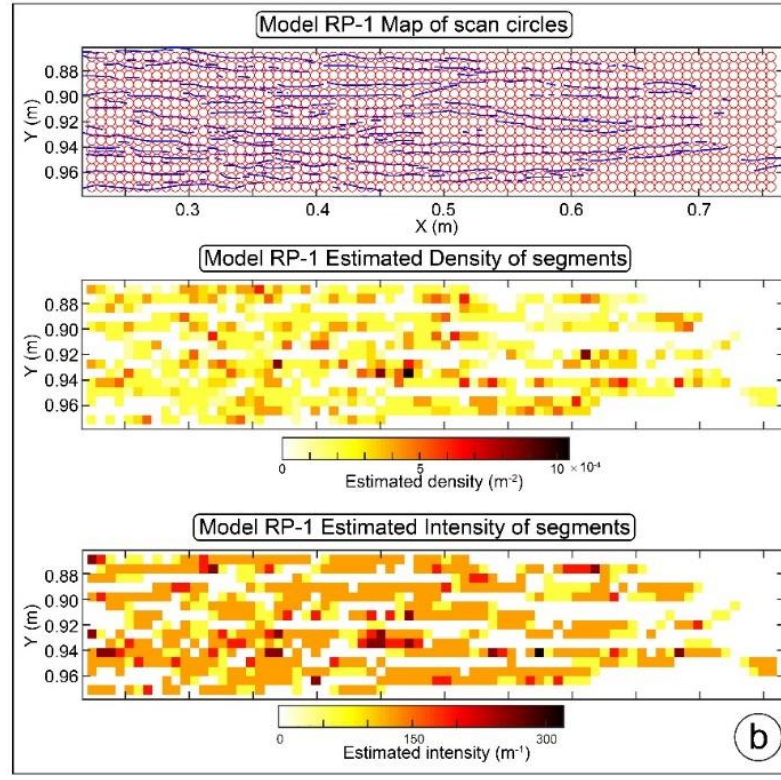




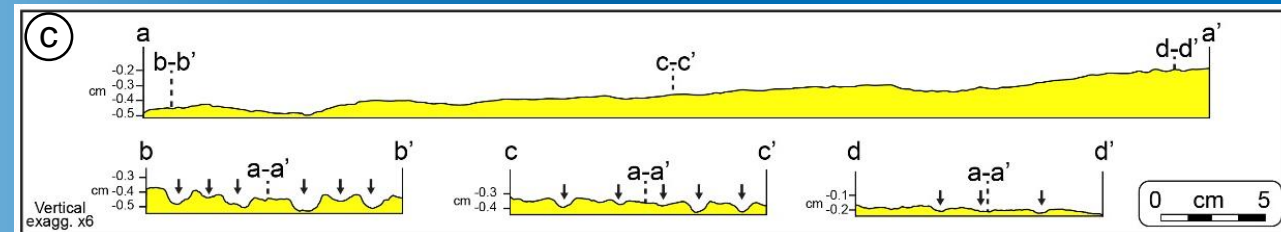
## REFERENCE MODEL (RP-1) :NO DISCONTINUITIES



(a) Graph showing the decrease of n. of grabens, their depth and width toward the proximal area of Model RP-1 (modified from Maestrelli et al., submitted).



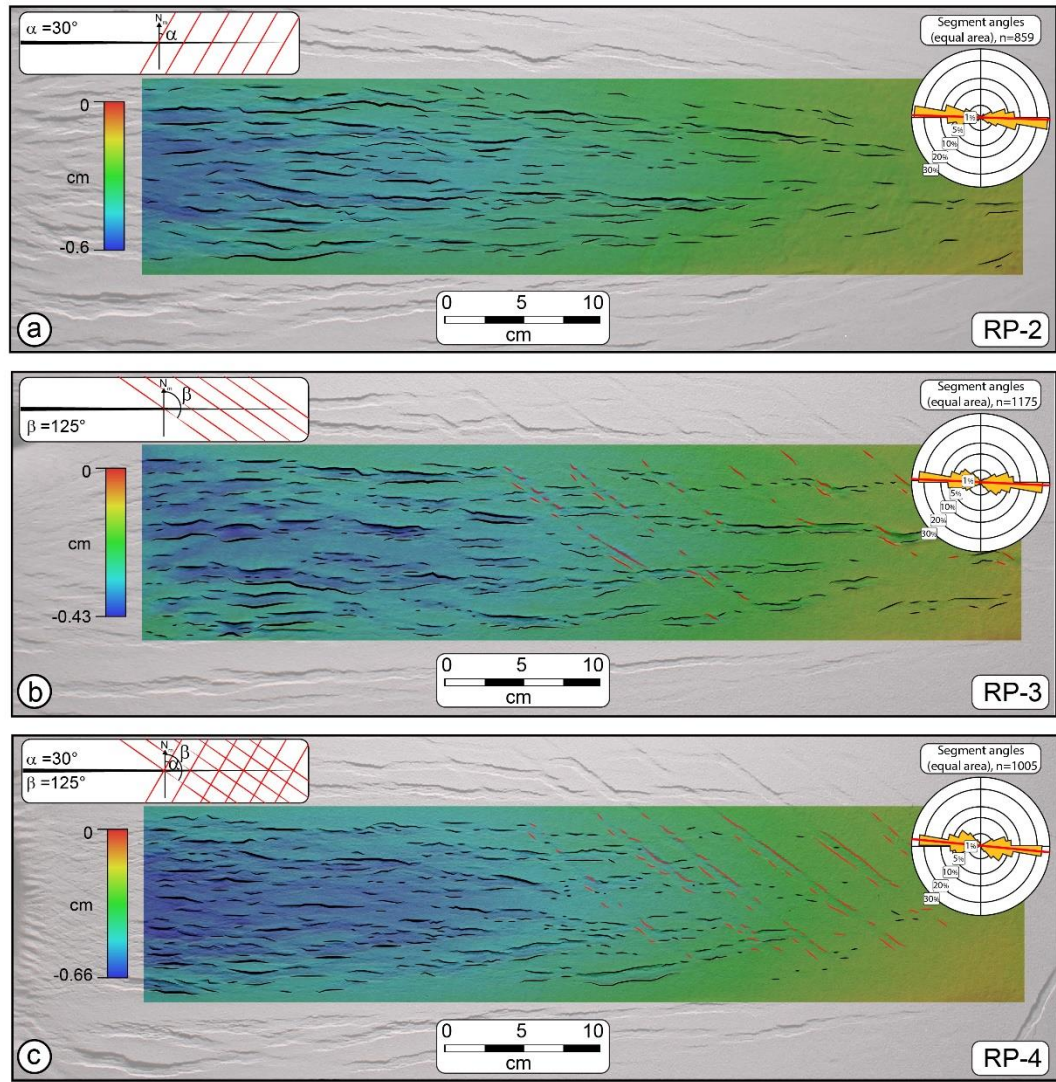
- Grabens forming in the distal area of the model are the first to be created by moving plate rotation, and show a larger subsidence. Topographic profiles b-b' orthogonal, to the direction of rift propagation (d), shows the presence of six main grabens. Graben number progressively decreases in profile c-c' and d-d', as well as graben width and depth (a). Fault density is higher in the distal and central areas of the model, while it is reduced in the proximal area (b).



(c) Topographic profiles across Model RP-1. Locations are shown in previous slide. (modified from Maestrelli et al., submitted).



## MODEL RP-2 to RP-4: $\alpha=30^\circ$ ; $\beta=125^\circ$

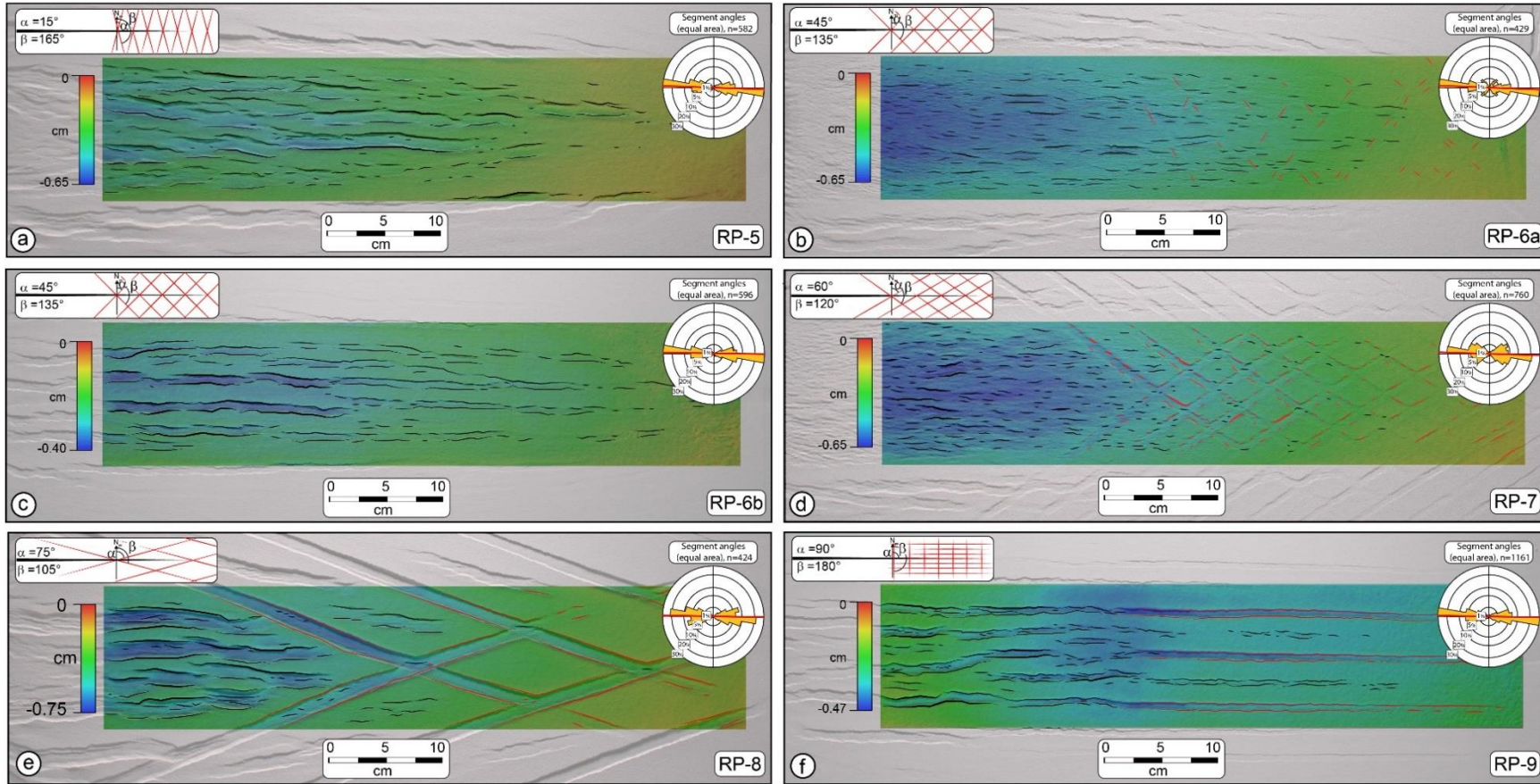


- Model RP-2, RP-3 and RP-4 (a to c) were designed to test the role of two sets of discontinuities in combination or one by one. Tested discontinuities trends with angles of  $\alpha=30^\circ$  (set S1) and  $\beta=125^\circ$ .
- In these models the general development did not differ from the evolution of model RP-1, showing incipient normal faulting in the proximal area of the model, which progressively propagated toward the rotation to form a “V-shaped” subsiding wedge in the centre of the model. The wedge tip migrated progressively with the opening of the metal plates. Model deformation showed a clear gradient in terms of fault throw and fault number (both larger for faults on the distal part of the model). The average fault trend is N90°.
- Interestingly, discontinuities trending with  $\beta=125^\circ$  were clearly reactivated (red lines in b,c) while no evidence of reactivation of set S1 ( $\alpha=30^\circ$ ) discontinuities was observed.

(a) Model RP-2 (b) Model RP-3 and (c) Model RP-4 top view evolution, showing a similar structural pattern to Model RP-1 and clear reactivation of discontinuity set S2 ( $\beta=125^\circ$ ; red lines). No reactivation of set S1 ( $\alpha=30^\circ$ ) was observed. (modified from Maestrelli et al., submitted).



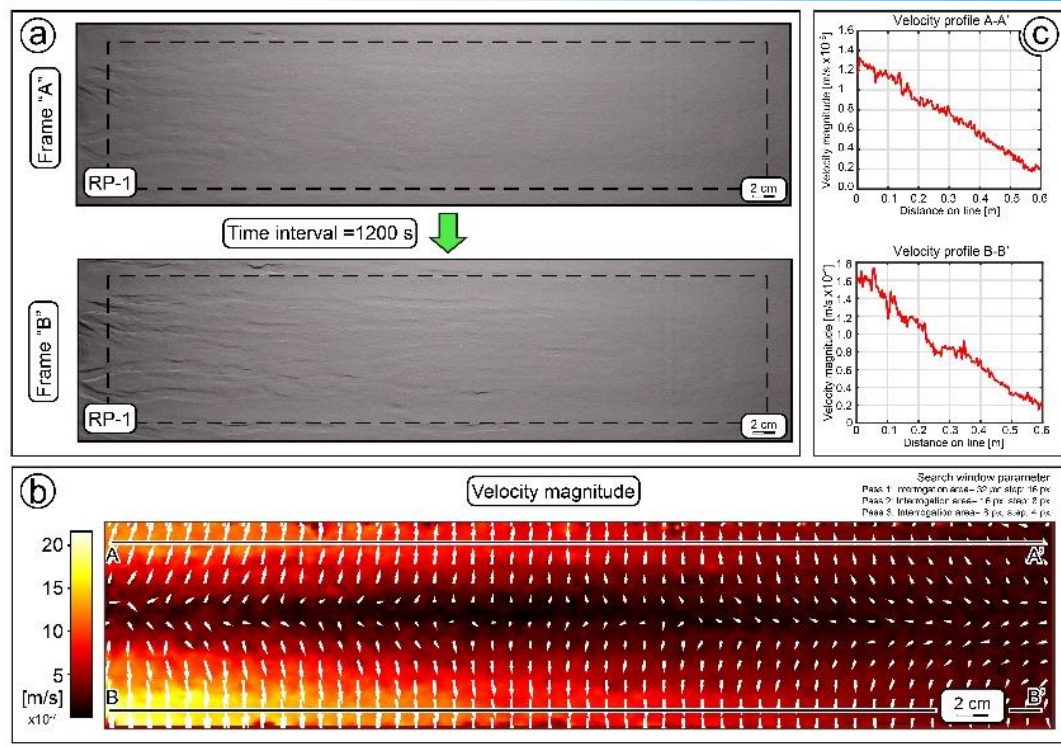
## MODEL RP-5 to RP-9: $\alpha$ and $\beta$ with various trend



(a to f) Model RP-5 to Model RP-9 top view evolution. No Reactivation is visible in Model RP-5 ( $\alpha=15^\circ$ ;  $\beta=165^\circ$ ; a). Clear reactivation of discontinuity sets S1 and S2 (red lines) is visible in Models RP-7 to RP-9. Besides, ambiguous reactivation is observed in Model RP-6a,b ( $\alpha=45^\circ$ ;  $\beta=135^\circ$ ; b and c) (modified from Maestrelli et al., submitted).

- These models (RP-5 to RP-9, a to f) systematically tested discontinuities trending with different  $\alpha$  and  $\beta$ .
- While some trends did not show any evidence of reactivation (e.g., Model RP-5,  $\alpha=15^\circ$ ;  $\beta=165^\circ$ ; a) some other clearly had evidence of S1 and S2 trend reactivation (e.g., models RP-7 to RP-9; see respective trends in the figure).
- Beside, model RP-6 showed in different attempts unclear evidence for reactivation of sets S1 and S2 ( $\alpha=45^\circ$ ;  $\beta=135^\circ$ ; b and c).

## GENERAL ASPECTS

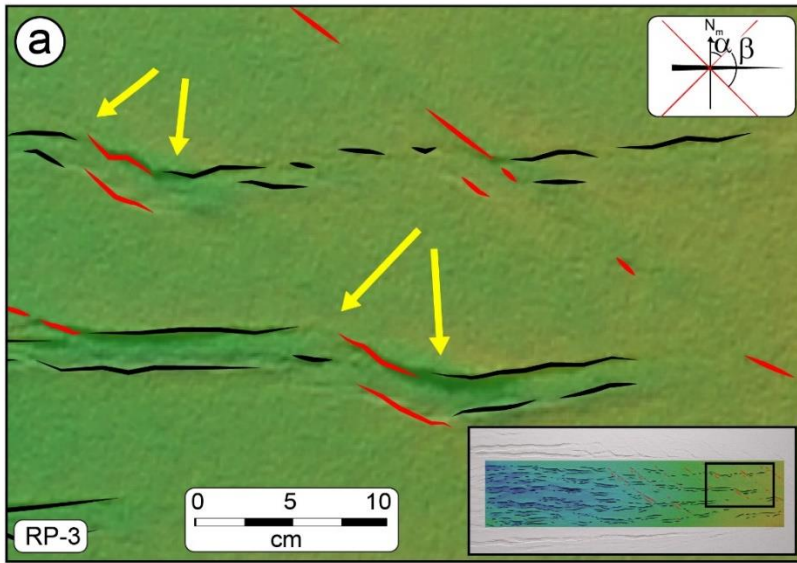


(a) Two target top-view photos (time interval 1200s) used to calculate vector displacement (using PIVlab software, Thielicke & Stamhuis, 2014) (modified from Maestrelli et al., submitted).

- Distribution and chronology of fault formation is in agreement with what expected from the adopted modelling strategy, whereby the rotational nature of the modelling setup implies a gradient of deformation propagating toward the poles of rotation.
- The gradient of vertical fault displacement is also consistently higher in the distal regions of the models (where cumulative deformation is larger) and smaller in distal areas adjacent to the rotation poles, which experience lower deformation.
- This behaviour is in agreement with the velocity pattern highlighted by DPIV analysis, marking a decreasing velocity gradient toward the poles of rotation (a,b,c). This pattern was observed in other models reproducing rotational rifting, such as the models by Zwaan et al. (2019). The presence of inherited brittle discontinuities in our experimental series represents a difference.
- Nonetheless, the role of inherited fabrics was also addressed by Molnar et al (2017, 2018, 2019). Despite a different aim and modelling setup, the overall surface deformation compares well with our models, as both show a “V-shaped” system of extensional faults with a clear decreasing gradient of deformation toward the rotation poles.



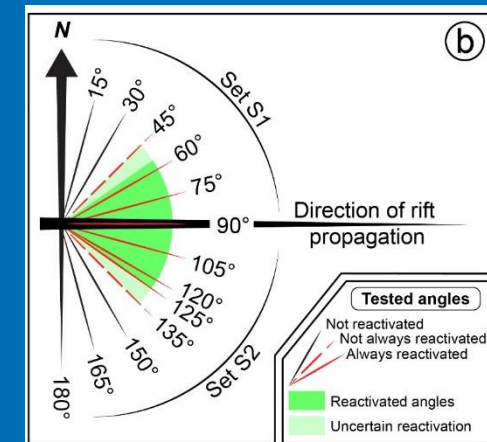
## EFFECT OF RIFT PROPAGATION ON INHERITED FABRICS



(a) Example of reactivated structures acting as transfer zones in Model RP-3 (modified from Maestrelli et al., submitted).

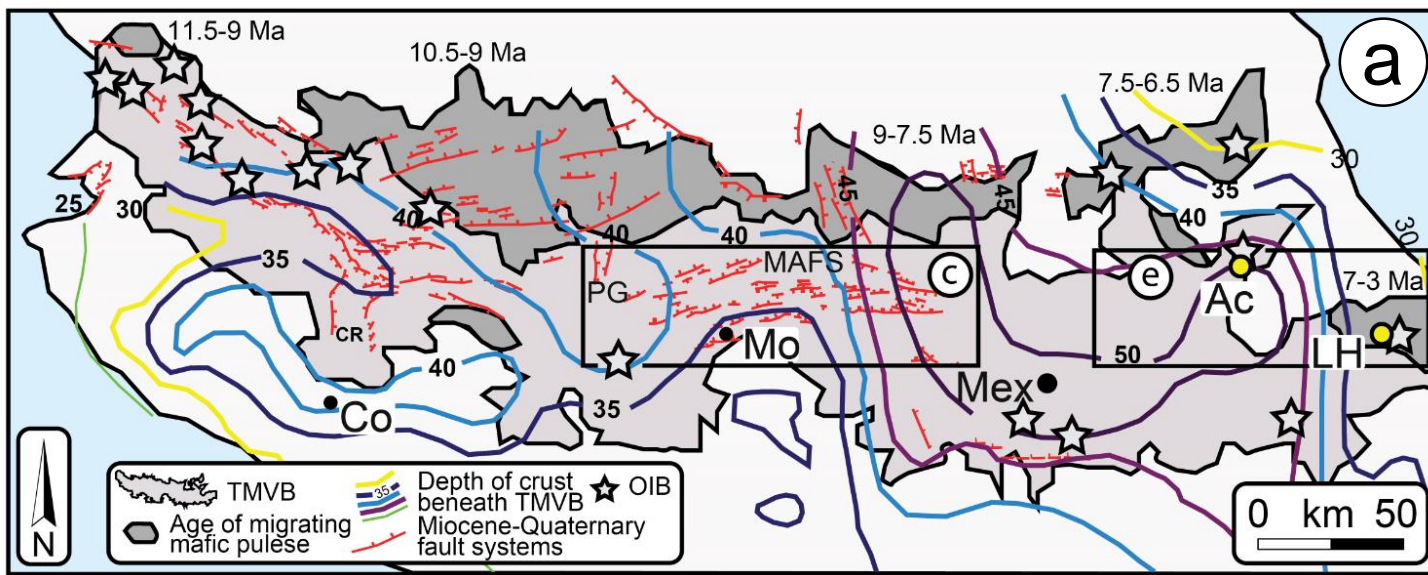
- Interesting is the effect of reactivated brittle (crustal) weak-zones in our models. Many rift-related faults (i.e., the black lines in a), were influenced by the reactivation of discontinuities.
- Remarkable is the effect of discontinuity set S2 trending at  $\alpha=125^\circ$  that interacted with the rift-related faults during their propagation, deflecting their trajectory (a). Reactivated structures acted as transfer zones, forcing the propagation of rift-related faults to shift laterally (yellow arrows in a).
- In other models, discontinuities trending to low-angle to the direction of rift propagation, them being reactivated as highly dilatant structures, inhibited the propagation of rift-related faults (e.g., in model RP-8).

- There is a clear relationship between the trend of discontinuities and their reactivation (a): only discontinuities ranging between  $\alpha=45^\circ$  and  $\beta=135^\circ$  are favourably oriented for being reactivated (b).
- Angles tested in Model RP-6 (i.e., set S1 trending  $a=45^\circ$  and set S2 trending  $b=135^\circ$ ) likely represent “limit angles” for reactivation, since out of the three models performed with this setup, two were not reactivated and only a single one (i.e., Model RP-6a) showed slight reactivation.
- This behaviour is confirmed by the observation that no reactivation has been observed for discontinuities trending with an angle  $a < 30^\circ$  and  $b > 135^\circ$  (b).



(b) Reactivated angles (modified from Maestrelli et al., submitted).

## COMPARISON WITH THE TMVB



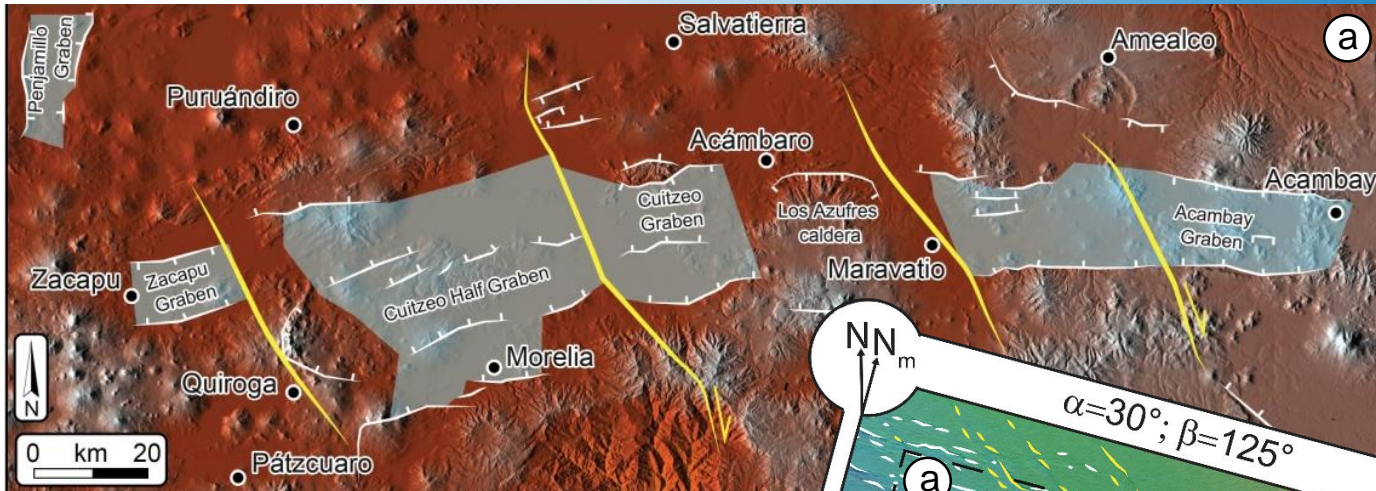
(a) TMVB and its extension through the North America plate. The two insets mark the position of the study areas. (modified from Maestrelli et al., submitted)

- Ferrari et al. (2012) showed how the crustal thickness doubles from W-NW toward E-SE, reaching the maximum value below Mexico City (a). Such an increase was also observed in our model, where analogue crust thickness is higher toward the area adjacent to the poles of rotation

- Similarities were also observed comparing extensional tectonic structures, showing a trend roughly parallel to the direction of rift propagation, with some major exceptions represented by ~N-S-trending structural systems (e.g., the Colima Rift and the Penajmillo Graben; a).
- Furthermore, fault density is higher in the area where crustal extension was originated, while less deformation is observed toward SE, where no NW-SE trending structure are observed at surface. This is in agreement with the pattern of deformation reproduced by our models



## COMPARISON WITH THE MAFS



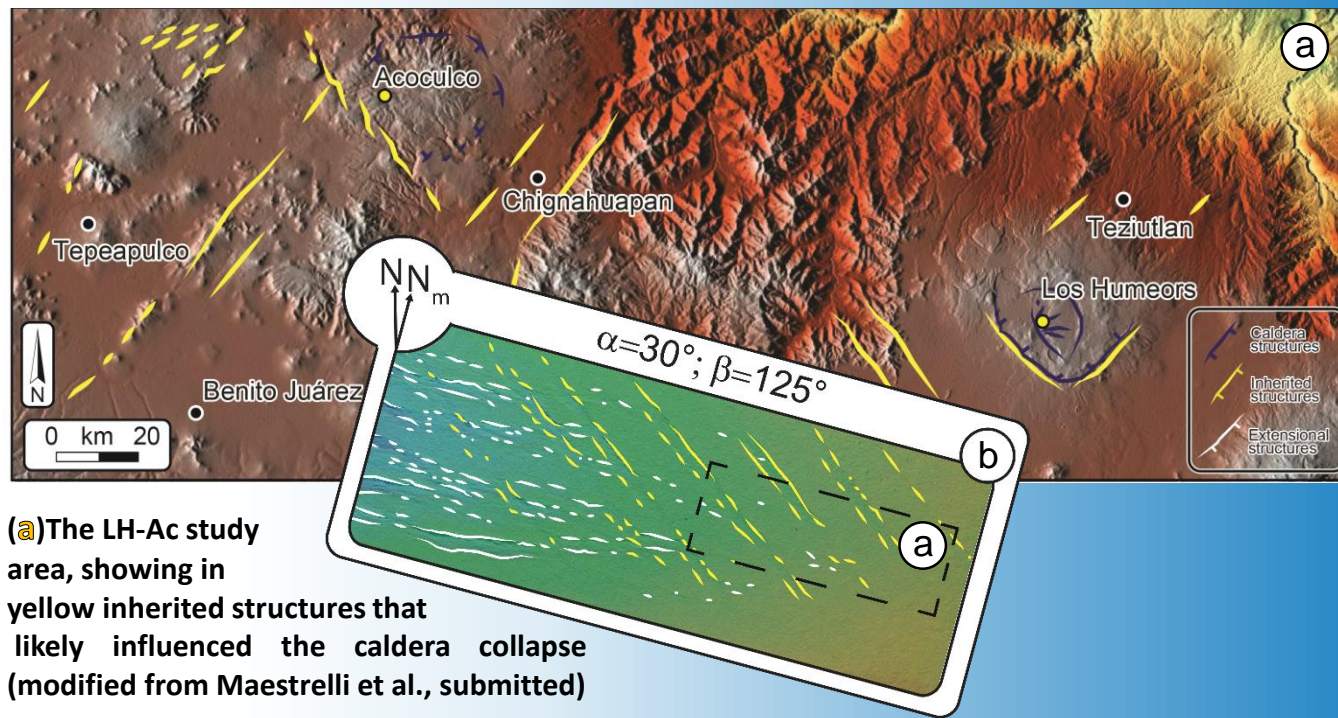
(a) The Morelia-Acambay Fault system (MAFS) in the central TMVB (modified from Maestrelli et al., submitted)

- Models RP-6a,b showed that a discontinuity with  $\beta=135^\circ$  is close to the boundary of reactivation, and can only occasionally be reactivated by extension propagation, while discontinuities trending  $\beta=125^\circ$  are invariably reactivated. This is in good agreement with the setting of the MAFS, which has been interpreted as a reactivated fault system (Garduño-Monroy et al., 2009).
- Fault reactivation can be related to rift-related extensional faulting. Model RP-4 (as well as others, e.g., Model RP-3) showed that inherited faults are often reactivated with a strike-slip component, which may offset the E-W fault pattern.

- The Morelia-Acambay Fault System (MAFS) shows important similarities with our models: a system of roughly E-W-trending Miocene-Quaternary grabens (white lines in a) are dissected by older ( $\sim 30$  Ma) NW-SE trending faults (yellow lines in a), which show evidence of right-lateral reactivation (Garduño-Monroy et al., 2009).
- In order to compare our models with nature, we have rotated the model to fit the geographic north (b). The trend of the MAFS faults is comparable to that of discontinuities S2 tested in Model RP-4 (anisotropies trending  $\beta=125^\circ$  in the model that corresponds to an azimuth N140° in nature) and Models RP-6a,b (anisotropies trending  $\beta=135^\circ$  in the model that correspond to an azimuth of N150° in nature).



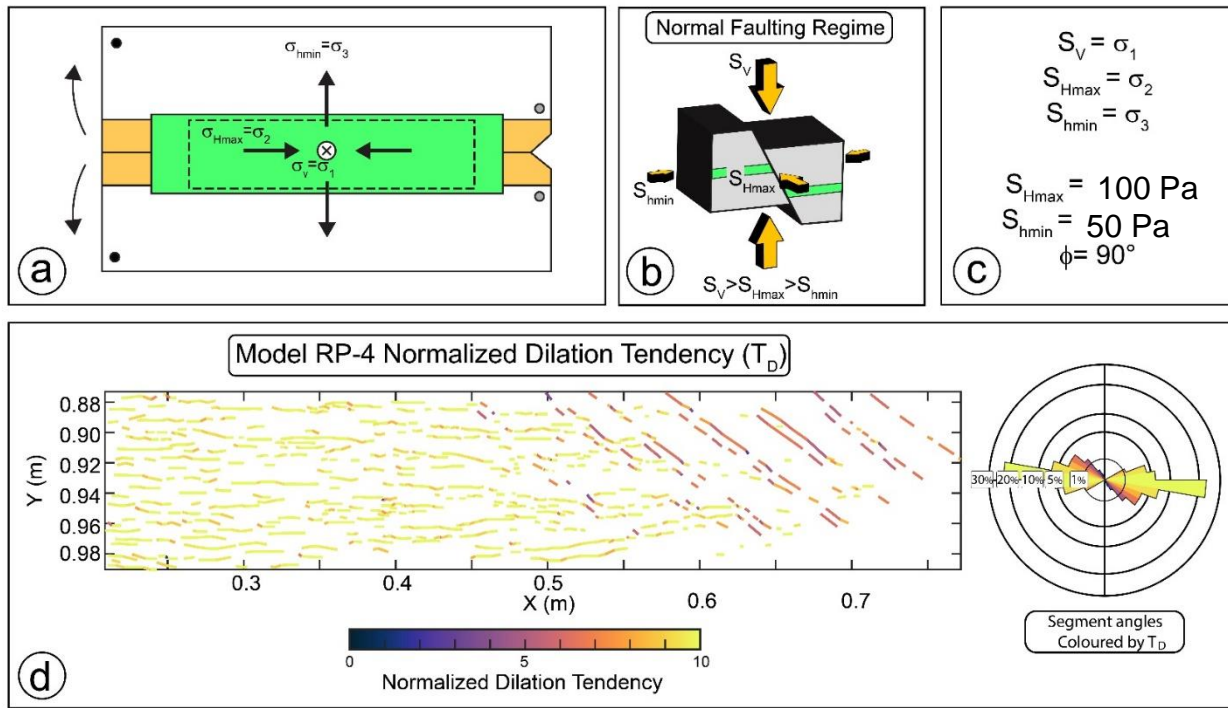
## COMPARISON WITH LH AND Ac CALDERA AREAS: INSIGHTS INTO GEOTHERMAL ASPECTS



(a) The LH-Ac study area, showing in yellow inherited structures that likely influenced the caldera collapse (modified from Maestrelli et al., submitted)

- Inherited crustal fabrics are reported in the Los Humeros and Acoculco area (a), where two trends of discontinuities striking on average N45° and N140° are observed at Acoculco and Los Humeros (Campos-Enriquez & Garduño-Monroy, 1987; Carrasco-Núñez et al., 2017; Avellán et al., 2019; García-Palomo et al., 2018).
- These structures may have played an important role in the localization of volcanic and caldera complex systems. Here, magma and associated geothermal fluids might have migrated exploiting secondary permeability associated with the existing structures.
- Applying the counter-clockwise rotation of 15° to the model (b), we obtain  $\alpha=30^\circ$  and  $\beta=135^\circ$  for discontinuities S1 and S2, respectively. These values were tested in Model RP-4, which showed that discontinuity set S2 was reactivated by crustal extension induced by the rift propagation.
- This implies that in this area the discontinuities trending around N140° might have been reactivated. This result accords well with the observation that the NW-SE trending faults in the Acoculco caldera system show the highest alteration produced by circulation of geothermal fluids (Liotta & WP4 Working Group, 2019).
- A further observation based on modelling results is that the interaction between rift-related faults and inherited fabrics may provide an efficient process for producing intersecting active structures, which provide favourable conditions for localising volcanic centres.

# COMPARISON WITH LH AND Ac CALDERA AREAS: INSIGHTS INTO GEOTHERMAL ASPECTS



(a) Stress field acting on models. (b) Theoretical stress field inducing a normal faulting regime. (c) Standard stress conditions assumed for the analysis of dilation tendency. (d) Normalized  $T_D$  for Model RP-4, calculated using FracPaQ software (Healy & Rizzo, 2017).

- Fault reactivation can be also analysed in terms of Dilation tendency (a to d). Normalized Dilation tendency ( $T_D$ ; Ferril et al., 1999) was tested on the faults of Model RP-4, by applying a scaled standard stress field compatible with crustal stretching imposed by model deformation (b, c).
- As expected, the most dilatant structures ( $T_D=1$ ) are the W-E trending normal faults which developed as a direct effect of the imposed stress field.
- Nonetheless,  $T_D$  analysis shows that also reactivated discontinuities of set S2 may experience some dilation (with values sometimes being  $>8$ ), especially in the area of linkage with rift-related faults (marked by warm colours in d).

- Even if we cannot consider the Dilation tendency ( $T_D$ ) of a structure as a direct proxy for permeability, the propensity of a structure to be opened can represent a favourable condition for channelling upward magmatic fluids, which may in turn localize eruptive centres.
- This observation is in agreement with the hypothesis that Los Humeros and Acoculco calderas are bounded by inherited rectilinear structures (e.g., Carrasco-Núñez et al., 2017) that might have favoured magma emplacement.



## ... SOME REMARKS

- Our parametric study explored the relationships between a propagating continental rift and the existing crustal discontinuities. Trend of structures with respect to the orthogonal to rift propagation (i.e., the initial  $\sigma_3$  axis) was systematically varied.
- Our models reproduced satisfactorily rift propagation in terms of density of structures, number and depth of grabens, and overall crustal thinning toward the pole of rotation. Models are comparable in general terms with existing processes described in the literature.
- The results of modelling provide new insights into the reactivation of inherited fabrics, suggesting that the reactivation field is delimited by angle  $\geq 45^\circ$  to the orthogonal to rift propagation.
- Depending on their orientation, reactivated inherited faults are often acting as transfer faults or oblique-slip faults. These features have the ability to offset rift propagation, generating fault patterns similar to some natural examples in the TMVB.
- Our analysis confirms that rift propagation may control both the large-scale and local-scale deformation patterns along the TMVB.
- Large-scale similarities can be found when comparing our models to the Trans-Mexican Volcanic Belts, as well as to the local-scale setting of the Morelia Acambay Fault System and the Los Humeros and Acoculco areas. Here, inherited discontinuities are reactivated as transfer faults and may interact with rift-related faults.
- Our analysis confirms that reactivated structure bear the potential to become preferential pathways for magma emplacement, therefore localizing volcanic centres and, afterward, the migration of geothermal fluids.



Los Humeros power plant. Source: <http://www.gemex-h2020.eu>

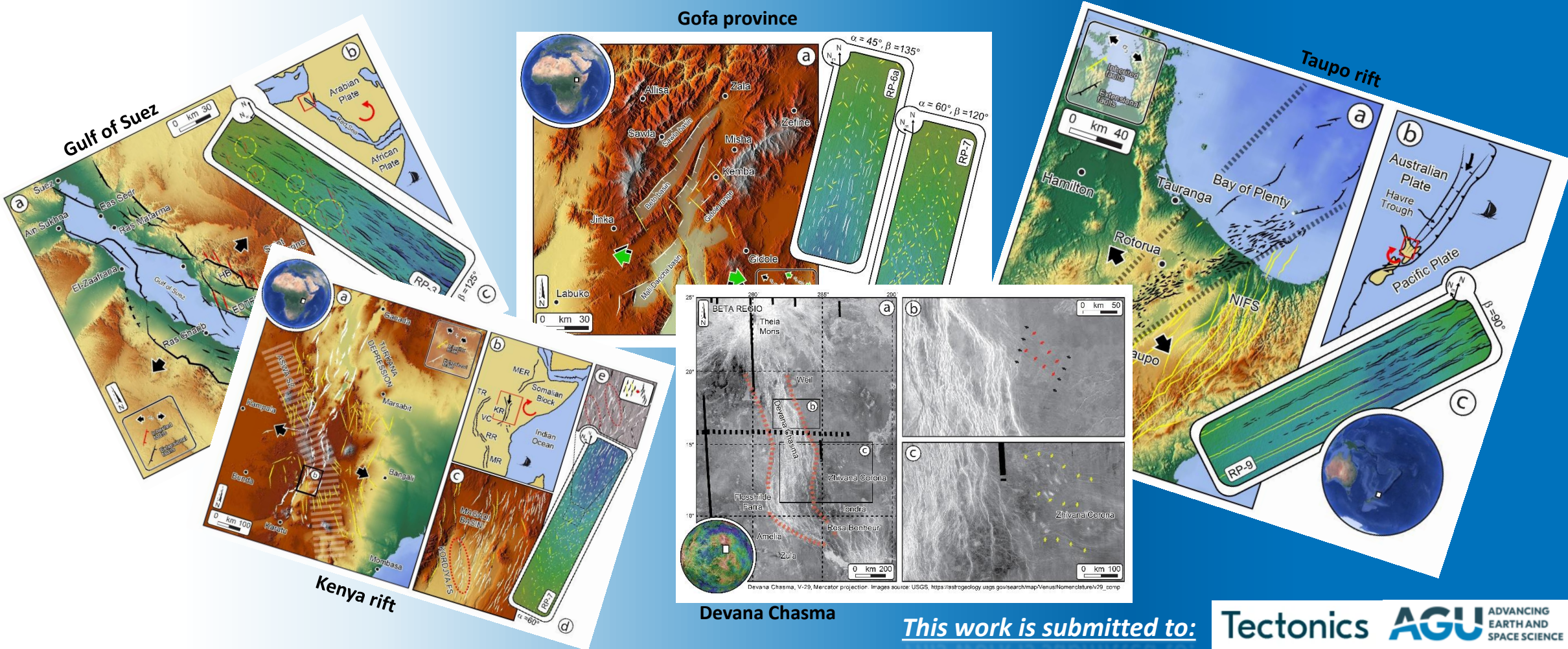


**NB: our models show similarities with many other natural prototypes...This aspect is addressed in the submitted paper!**



# ... SOME MORE EXAMPLES

- In our submitted paper we compare our models to other natural examples, focusing on the interaction between propagating rift systems and inherited crustal fabrics...we hope to show you this soon!



This work is submitted to: **Tectonics** **AGU** ADVANCING EARTH AND SPACE SCIENCE



- Avellán, D. R., Macías, J. L., Layer, P. W., Cisneros, G., Sánchez-Núñez, J. M., Gómez-Vasconcelos, M. G., Pola, A., Sosa-Ceballos, G., García-Tenorio, F., Reyes Agustín, G., Osorio-Ocampo, S., García-Sánchez, L., Mendiola, I.F., Marti, J., López-Loera H., Benowitz, J. (2019). Geology of the late Pliocene–Pleistocene Acoculco caldera complex, eastern Trans-Mexican Volcanic Belt (México). Journal of Maps, 15(2), 8-18. <https://doi.org/10.1080/17445647.2018.1531075>
- Campos-Enriquez, J., & Garduño-Monroy, V. H. (1987). The shallow structure of Los Humeros and Las Derrumbadas geothermal fields, Mexico. Geothermics, 16(5-6), 539-554. [https://doi.org/10.1016/0375-6505\(87\)90038-1](https://doi.org/10.1016/0375-6505(87)90038-1)
- Carrasco-Núñez, G., López-Martínez, M., Hernández, J., & Vargas, V. (2017). Subsurface stratigraphy and its correlation with the surficial geology at Los Humeros geothermal field, eastern Trans-Mexican Volcanic Belt. Geothermics, 67, 1-17. <http://dx.doi.org/10.1016/j.geothermics.2017.01.001>
- Del Ventisette, C., Bonini, M., Agostini, A., Corti, G., Maestrelli, D., & Montanari, D. (2019). Using different grain-size granular mixtures (quartz and K-feldspar sand) in analogue extensional models. Journal of Structural Geology, 129, 103888. <https://doi.org/10.1016/j.jsg.2019.103888>
- Ferrari, L. (2004). Slab detachment control on mafic volcanic pulse and mantle heterogeneity in central Mexico. Geology, 32(1), 77-80. Ferrari, L. (2004). Slab detachment control on mafic volcanic pulse and mantle heterogeneity in central Mexico. Geology, 32(1), 77-80. <https://doi.org/10.1130/G19887.1>
- Ferrari, L., Orozco-Esquivel, T., Manea, V., & Manea, M. (2012). The dynamic history of the Trans-Mexican Volcanic Belt and the Mexico subduction zone. Tectonophysics, 522, 122-149. <https://doi.org/10.1016/j.tecto.2011.09.018>
- Ferrill, D.A., Winterle, J., Wittmeyer, G., Sims, D., Colton, S., Armstrong, A. & Morris, A.P. (1999). Stressed rock strains groundwater at Yucca Mountain, Nevada. GSA Today, 9(5), pp.1-8.
- García-Palomo, A., Macías, J. L., Jiménez, A., Tolson, G., Mena, M., Sánchez-Núñez, J. M., ... & Lermo-Samaniego, J. (2018). NW-SE Pliocene-Quaternary extension in the Apan-Acoculco region, eastern Trans-Mexican Volcanic Belt. Journal of Volcanology and Geothermal Research, 349, 240-255. <https://doi.org/10.1016/j.jvolgeores.2017.11.005>
- Garduño-Monroy et al., 2009 Garduño-Monroy, V. H., Pérez-Lopez, R., Israde-Alcantara, I., Rodríguez-Pascua, M. A., Szyrkaruk, E., Hernández-Madrigal, V. M., ... & García-Estrada, G. (2009). Paleoseismology of the southwestern Morelia-Acambay fault system, central Mexico. Geofísica internacional, 48(3), 319-335.
- Healy, D., Rizzo, R. E., Cornwell, D. G., Farrell, N. J., Watkins, H., Timms, N. E., ... & Smith, M. (2017). FracPaQ: A MATLAB™ toolbox for the quantification of fracture patterns. Journal of Structural Geology, 95, 1-16. <https://doi.org/10.1016/j.jsg.2016.12.003>
- Liotta, D., and WP4 Working Group, (2019). Final report on active systems: Los Humeros and Acoculco. Deliverable 4.1, GEMex project, European Union's Horizon 2020 programme, 334 pp.
- Maestrelli, D., Montanari, D., Corti, G., Del Ventisette, C., Moratti, G., Bonini, M. (submitted to Tectonics). Exploring the interactions between rift propagation and inherited crustal fabrics through experimental modelling.
- Molnar, N. E., Cruden, A. R., & Betts, P. G. (2017). Interactions between propagating rotational rifts and linear rheological heterogeneities: Insights from three-dimensional laboratory experiments. Tectonics, 36(3), 420-443. <https://doi.org/10.1002/2016TC004447>
- Molnar, N. E., Cruden, A. R., & Betts, P. G. (2018). Unzipping continents and the birth of microcontinents. Geology, 46(5), 451-454. <https://doi.org/10.1130/G40021.1>
- Molnar, N. E., Cruden, A. R., & Betts, P. G. (2019). Interactions between propagating rifts and linear weaknesses in the lower crust. Geosphere. <https://doi.org/10.1130/GES02119.1>
- Montanari, D., Agostini, A., Bonini, M., Corti, G., & Ventisette, C. (2017). The use of empirical methods for testing granular materials in analogue modelling. Materials, 10(6), 635.
- Thielicke, W and Stamhuis, E J (2014) PIVlab – Towards User-friendly, Affordable and Accurate Digital Particle Image Velocimetry in MATLAB. Journal of Open Research Software, 2: e30, DOI: <http://dx.doi.org/10.5334/jors.bl>
- Zwaan, F., Schreurs, G., & Rosenau, M. (2019). Rift propagation in rotational versus orthogonal extension: Insights from 4D analogue models. Journal of Structural Geology, 103946. <https://doi.org/10.1016/j.jsg.2019.103946>

## ACKNOWLEDGMENTS

This work has been performed in the frame of the **GEMex Project-Cooperation in Geothermal energy research Europe-Mexico for development of Enhanced Geothermal Systems and Superhot Geothermal Systems**



(Horizon 2020 Programme, grant agreement No. 727550). We kindly acknowledge the Europe-Mexico consortium and all the GEMex partners for providing support to this research.



## DANIELE MAESTRELLI



CNR-IGG The National Research Council of Italy,  
Institute of Geosciences and Earth Resources,  
Florence, Italy

E-mail: [daniele.maestrelli@igg.cnr.it](mailto:daniele.maestrelli@igg.cnr.it)  
[daniele.maestrelli@gmail.com](mailto:daniele.maestrelli@gmail.com)

- *Daniele is a post-doc research fellow at the IGG-CNR, Florence.*
- *His interests are related to structural geology, analogue modelling, seismic interpretation, mud volcanism and fluid migration.*

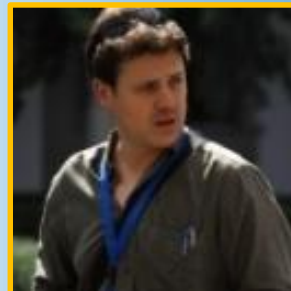
## MARCO BONINI



CNR-IGG The National Research Council of Italy,  
Institute of Geosciences and Earth Resources,  
Florence, Italy

E-mail: [marco.bonini@igg.cnr.it](mailto:marco.bonini@igg.cnr.it)  
[marco.bonini27@gmail.com](mailto:marco.bonini27@gmail.com)

## DOMENICO MONTANARI



CNR-IGG The National Research Council of Italy,  
Institute of Geosciences and Earth Resources,  
Florence, Italy

E-mail: [domenico.montanari@igg.cnr.it](mailto:domenico.montanari@igg.cnr.it)

## GIACOMO CORTI



CNR-IGG The National Research Council of Italy,  
Institute of Geosciences and Earth Resources,  
Florence, Italy

E-mail: [Giacomo.Corti@igg.cnr.it](mailto:Giacomo.Corti@igg.cnr.it)

## GIOVANNA MORATTI



CNR-IGG The National Research Council of Italy,  
Institute of Geosciences and Earth Resources,  
Florence, Italy

E-mail: [giovanna.moratti@igg.cnr.it](mailto:giovanna.moratti@igg.cnr.it)

